JOURNAL OF GENERAL VIROLOGY

RESEARCH ARTICLE

Pang *et al.*, *Journal of General Virology* 2019;100:999–1012

DOI 10.1099/jgv.0.001243

MICROBIOLOGY SOCIETY

OPEN MICROBIOLOGY

Defining early events of Epstein–Barr virus (EBV) infection in immortalized nasopharyngeal epithelial cells using cell-free EBV infection

Pei Shin Pang,[1]† Tengfei Liu,[1]† Weitao Lin,[1] Chi-Man Tsang,[1,2] Yim-Ling Yip,[1] Yuan Zhou,[1] Xin-Yuan Guan,[3] Ronald Cheong-Kin Chan,[2] Sai-Wah Tsao[1,*] and Wen Deng[4,*]

Abstract

Epstein–Barr virus (EBV) infection is strongly associated with nasopharyngeal carcinoma, a common cancer in Southeast Asia and certain regions of Africa. However, the dynamics of EBV episome maintenance in infected nasopharyngeal epithelial (NPE) cells remain largely undefined. Here, we report the establishment of a highly efficient cell-free EBV infection method for NPE cells. By using this method, we have defined some of the dynamic events involved in the early stage of EBV infection in NPE cells. We report, for the first time, a rapid loss of EBV copies from infected NPE cells during the first 12–72 h post-infection. The rate of EBV loss slowed at later stages of infection. Live cell imaging revealed that the freshly infected NPE cells were delayed in entry into mitosis compared with uninfected cells. Freshly infected NPE cells transcribed significantly higher levels of lytic EBV genes *BZLF1* and *BMRF1* yet significantly lower levels of *EBER1/2* than stably infected NPE cells. Notably, there were very low or undetectable levels of protein expressions of *EBNA1*, *LMP1*, *Zta* and *Rta* in freshly infected NPE cells, whereas *EBNA1* and *LMP1* proteins were readily detected in stable EBV-infected NPE cells. The kinetics of EBV loss and the differential EBV gene expression profiles between freshly and stably infected NPE cells are in line with the suggestion of epigenetic changes in the EBV genome that affect viral gene expression and the adaptation of host cells to EBV infection to maintain persistent EBV infection in NPE cells.

INTRODUCTION

Nasopharyngeal carcinoma (NPC) is prevalent in Southeast Asia and certain regions of Africa, with a particularly high incidence in southern China including Hong Kong [1]. Epstein–Barr virus (EBV) infection has been postulated to be an important aetiological factor in the pathogenesis of NPC. Undifferentiated NPC, the major histological type of NPC in endemic regions, is universally associated with EBV infection [1]. Clonal EBV infection has also been found in pre-invasive lesions of the nasopharynx, suggesting that the focal deregulated cellular growth may arise from clonal expansion of a single EBV-infected premalignant nasopharyngeal epithelial (NPE) cell, supporting a role for EBV infection in the early process of NPC development [2]. Unlike the situation in B cells, infection of epithelial cells with EBV has been difficult to achieve in culture. Hence, the early events involved in infection of premalignant NPE cells have been difficult to investigate and remain largely unknown. The cell-to-cell contact mode of infection, by co-culturing epithelial cells with EBV-infected B cells (e.g. EBV-infected Akata cells) induced to undergo lytic reactivation of EBV, has overcome this obstacle in infecting epithelial cells [3–5]. However, the EBV-producing Akata cells establish tight junctional conjugates with the co-culturing epithelial cells and are difficult to separate from epithelial cells after co-culture. The association of EBV-producing Akata cells with the infected epithelial cells prevents accurate investigation of early events of EBV infection in epithelial cells, such as profiles of EBV gene expression and dynamics of EBV copy number changes in freshly infected epithelial cells. Cell-free infection is an alternative approach

Received 24 May 2018; Accepted 18 February 2019; Published 28 February 2019

Author affiliations: [1]School of Biomedical Sciences, Li Ka Shing Faculty of Medicine, The University of Hong Kong, Hong Kong, SAR, PR China; [2]Department of Anatomical and Cellular Pathology, The State Key Translational Laboratory, Faculty of Medicine, The Chinese University of Hong Kong, Hong Kong, SAR, PR China; [3]Department of Clinical Oncology, Li Ka Shing Faculty of Medicine, The University of Hong Kong, Hong Kong, SAR, PR China; [4]School of Nursing, Li Ka Shing Faculty of Medicine, The University of Hong Kong, Hong Kong, SAR, PR China.

***Correspondence:** Sai-Wah Tsao, gswtsao@hku.hk; Wen Deng, wdeng@hku.hk

Keywords: Epstein–Barr virus; nasopharyngeal epithelial cells; cell-free infection; dynamics; early events; gene expression.

Abbreviations: EBV, Epstein–Barr virus; FISH, fluorescence *in situ* hybridization; FACS, fluorescence-activated cell sorting; GRU, green Raji unit; NPC, nasopharyngeal carcinoma; NPE, nasopharyngeal epithelial; MOI: multiplicity of infection.

†These authors contributed equally to this work.

Five supplementary figures and two supplementary tables are available with the online version of this article.

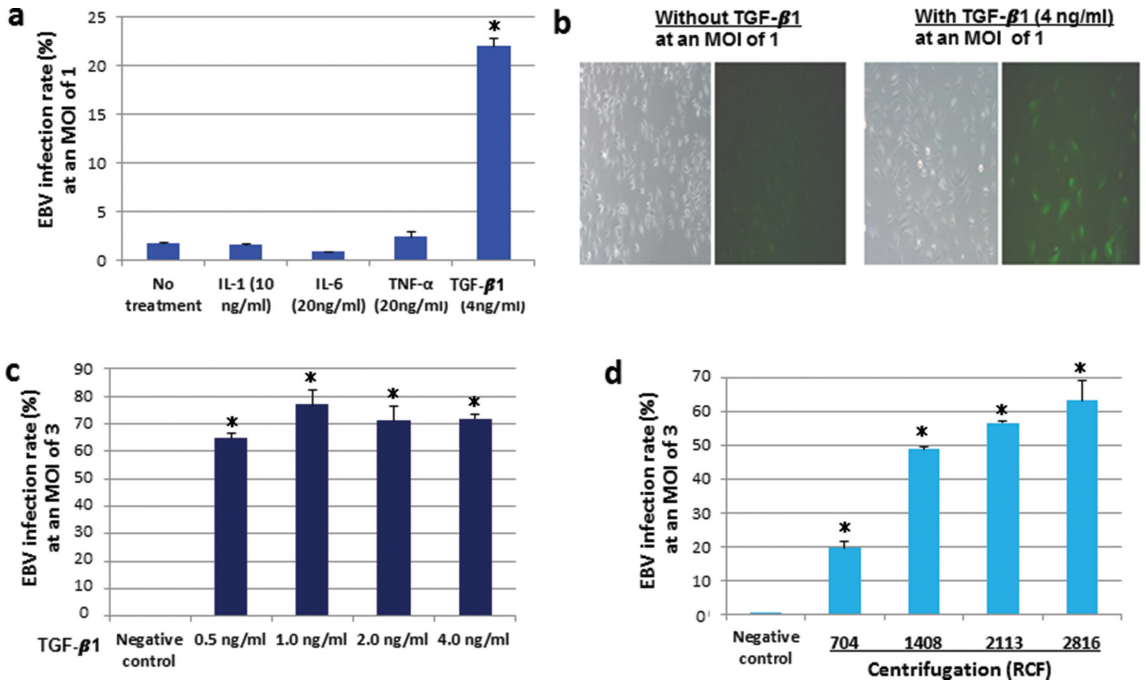

Fig. 1. The combination of TGF-β1 treatment and centrifugation greatly enhances EBV infection efficiencies in NPE cells. Data from NP460hTert cells are presented. EBV infection rates (percentages of GFP-positive cells) were analysed using flow cytometry 48 h after EBV infection. Error bars indicate standard deviations of triplicate experiments. (a) Comparison of the effectiveness of different cytokines at commonly used concentrations in affecting EBV infection rates under 2465 RCF centrifugation. *Significant difference (P<0.01) between TGF-β1 and other treatments. (b) Typical fluorescence images of NP460hTert cells 2 days after EBV infection with or without TGF-β1 treatment but with 2465 RCF centrifugation. GFP-positive cells represent EBV-infected cells. (c) TGF-β1 at concentrations of 0.5-4 ng ml^{-1} resulted in comparable effects in enhancing EBV infection efficiencies under centrifugation. *Significant difference (P<0.01) between each TGF-β1 treatment and negative control. (d) Centrifugation significantly enhances EBV infection efficiency in NPE cells under TGF-β1 treatment (2 ng ml^{-1}). *Significant difference (P<0.01) between each centrifugation and negative control. Note that centrifugation or TGF-β1 treatment alone [negative control in (c) and (d)] resulted in a very low efficiency of EBV infection.

for EBV infection of epithelial cells, but with a low efficiency of infection [3, 4]. In this study, we have developed a highly efficient method of cell-free EBV infection of immortalized NPE cells, and have applied it to characterize early events of EBV infection, which are poorly defined, in NPE cells. Immortalization is an early and indispensable step towards cancer development. Immortalized cells have been commonly used as premalignant cell models to study the early events leading to malignant transformation. The efficient EBV infection system of immortalized NPE cells using a cell-free infection approach will contribute to our understanding of events leading to establishment of stable EBV infection in NPE cells, which has been postulated to be an early and essential step in NPC development. In this study, we were able to achieve stable infection of EBV in immortalized NPE cells after multiple rounds of cell sorting by fluorescence-activated cell sorting (FACS). The freshly and stably EBV-infected NPE cells differed in their dynamics of EBV episome maintenance and viral gene expression. In particular, we observed a rapid decrease in the percentage of EBV-positive cells in freshly infected immortalized NPE cells within the first 72 h post-infection. Lytic EBV genes were transcribed at relatively high levels in freshly infected NPE cells but silenced in stably EBV-infected NPE cells. Additional novel and interesting findings include the lower levels of EBER1/2 transcription in freshly infected cells compared to stably infected counterparts and, most surprisingly, undetectable or very low levels of protein expression levels of analysed EBV latent and lytic genes despite the detection of mRNA transcription in freshly infected cells. Our results show that stable EBV infection in NPE cells is established from a small population of immortalized NPE cells and may involve adaptive interaction between EBV and the infected NPE cells to allow effective translation of latent EBV proteins from mRNA for viral maintenance and host cell expansion. Establishment of efficient cell-free infection of NPE cells and characterization of early events in EBV infection of NPE cells will facilitate investigation into the role of EBV infection in the pathogenesis of NPC.

RESULTS

Development of a high-efficiency method of cell-free EBV infection of NPE cells

While a cell-to-cell contact mode of infection has overcome the difficulty in infecting epithelial cells with EBV, the

difficulty in eliminating the EBV-producing B cells from co-culturing NPE cells hinders investigations to define early events of EBV infection of NPE cells. Previously published cell-free infection protocols could only achieve low EBV infection efficiencies in epithelial cells [3, 4]. We postulate that cytokines may play an important role in facilitating EBV infection of epithelial cells. We examined the potential of different cytokines to enhance the efficiency of cell-free EBV infection of NPE cells. In this study, we used Akata-EBV tagged with GFP to enable convenient identification of EBV-infected NPE cells. The infection rate of EBV could be conveniently monitored based on the percentage of GFP-positive NPE cells detected by flow cytometry. Among various cytokines examined (including IL-1, IL-6, TNF-α and TGF-β1), TGF-β1 pretreatment for 24 h was found to dramatically increase the EBV infection rate (indicated by the percentage of GFP-positive cells) in NPE cells using the cell-free infection method compared with the infection rate in control NPE cells without any treatment (P<0.01) (Fig. 1a, b). The effective concentrations of TGF-β1 ranged from 0.5 to 4 ng ml^{-1}, with similar effects in enhancing EBV infection efficiency (Fig. 1c). We also applied another independent method, EBV fluorescence *in situ* hybridization (FISH) using EBV-specific DNA probes, to determine if TGF-β1 pretreatment truly increases EBV infection efficiency in NPE cells. As shown in Fig. S1 ,available in the online version of this article, the percentages of EBV-positive cells and the average EBV copy numbers per cell detected using FISH in NPE cells with TGF-β1 pretreatment were significantly higher (P<0.01) than those without TGF-β1 pretreatment. Therefore, the finding that TGF-β1 pretreatment enhances EBV infection efficiency is consistent based on two different methods of EBV infection detection. Although GFP expression appears to be less sensitive than EBV FISH in detecting EBV infection, GFP expression can be used for convenient detection of infection in live cells, and thus was used to indicate EBV infection in some of our experiments. In addition to the pretreatment of NPE cells with TGF-β1, a centrifugation step (1408–2816 RCF for 1 h at 37 °C) after addition of EBV-containing supernatant onto the TGF-β1-treated NPE cells was also found to be essential to achieve the high infection rate of NPE cells (Fig. 1d). The centrifugation step probably involved spinning down the EBV-bound subcellular components in the culture supernatant onto the surface of NPE cells to facilitate viral entry into NPE cells. The optimized EBV infection protocols of the cell-free EBV infection method are described in detail in the Methods.

The efficiencies of the cell-free EBV infection were compared with the cell-to-cell contact mode of infection in three telomerase-immortalized NPE cell lines, NP361hTert, NP460hTert and NP550hTert (Fig. 2a, b), all of which were established in our laboratory [5–7]. TGF-β1 pretreatment enhanced the rates of EBV infection in both modes of infection. For NP361hTert and NP460hTert cell lines, the co-culture method of infection was more efficient than cell-free infection at an MOI of 2. It is clear that TGF-β1 treatment is essential for EBV infection of NPE cells via the cell-free infection protocol. The underlying mechanism for TGF-β1 treatment-enhanced EBV infection efficiency in the cell-free infection is currently under investigation, but may not involve epithelial differentiation as no consistent significant changes in cytokeratin profiles of NPE cells were detected after TGF-β1 treatment (Fig. S2).

Dynamics of EBV maintenance in infected NPE cells at the early stage of infection

EBV infection is universally present in undifferentiated NPC cells. Yet events involved in the early stages of EBV infection in NPE cells are largely unknown. Using the efficient cell-free infection method, we have defined some of the early events of EBV infection in NPE cells with aspects relating to cell cycle progression, dynamics of EBV maintenance and EBV gene expression profiles. Since Akata-EBV used in this study was tagged with GFP, we could also monitor the infection dynamics and growth behaviour of EBV-infected cells using live-cell imaging. The expression of GFP from Akata-EBV is driven by the SV40 promoter, which will only be activated after EBV particles have entered the cell nucleus. We observed that GFP expression could be detected as early as 12 h after infection of NPE cells, implying that a time interval of 12 h is required for EBV to enter the nucleus of an infected cell and to begin gene expression (Fig. 2c, d). In addition, we also performed EBV FISH to determine the percentage of EBV-infected NPE cells and dynamic changes of EBV copy numbers in nuclei of infected NPE cells at different time points post-infection at the single cell level. Using two telomerase-immortalized NPE cell models (NP361hTert and NP460hTert), we characterized the dynamics of EBV maintenance at early stages of EBV infection in NPE cells. In both immortalized NPE cell models, we observed rapid decreases in the percentages of EBV-infected cells as well as in average EBV copy numbers per cell within the first 72 h post-infection. As shown in Fig. 3(a), EBV copies were detected in ~80 % of NP460hTert cells at 12 h post-infection. However, the percentage of EBV-positive cells decreased rapidly to ~40 and ~20 % at 48 and 72 h post-infection, respectively. In another immortalized NPE cell line, NP361hTert, EBV infection was detected in ~60, ~40 and~20 % of the cells at 12, 48 and 72 h post-infection, respectively (Fig. 3d). In both cell lines, the rates of decrease in the percentages of EBV-positive cells became stabilized during the 96–144 h post-infection period. The dynamic changes in average EBV copy numbers per cell and average EBV copy numbers per EBV-positive cell at different time points after EBV infection are shown in Fig. 3(b, c, e, f). Clear trends of decrease in the average EBV copy numbers per cell were detected during the 12–72 h post-infection period in both cell lines. The rates of decrease in EBV copy numbers per cell also slowed down and stabilized during 96–144 h post-infection. Of note, the results of average EBV copy numbers per EBV-positive cell were an underestimation of the trend of EBV copy loss because the infected NPE cells, which had completely lost their EBV episomes, were not included in the calculation. Fig. 4 shows typical images

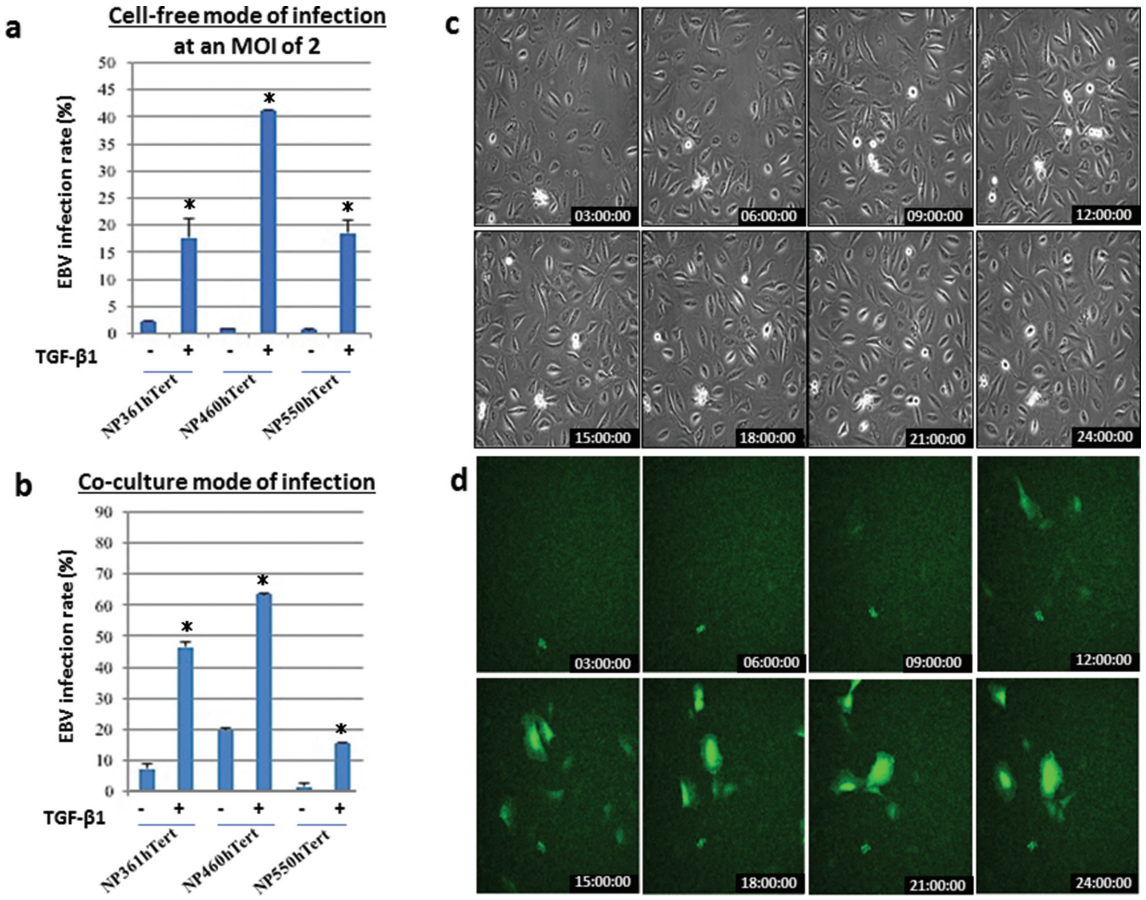

Fig. 2. TGF-β1 treatment enhances EBV infection efficiencies in various NPE cell lines. In (a) and (b), EBV infection rates (percentages of GFP-positive cells) were analysed using flow cytometry 48 h after EBV infection; error bars indicate standard deviations of triplicate experiments; *significant difference (P<0.01) between EBV infection rate with (+) and without (-) TGF-β1 treatment. (a) TGF-β1 treatment enhanced EBV infection rates in all three tested NPE cell lines using a cell-free mode of infection. (b) TGF-β1 treatment enhanced EBV infection rates in all three tested NPE cell lines using a cell-to-cell contact mode of infection. (c) Phase-contrast live cell images of NP460hTert cells at different time points post-infection. (d) Fluorescence images of the same field of cells at different time points post-infection as in (c). Each time point of imaging (hours:minutes:seconds) is given at the bottom right of each image. Note that clear GFP signals could be detected starting from 12 h post-infection.

of EBV FISH in NP460hTert and NP361hTert cells at 12 and 72 h post-infection and in stably infected cells. In general, our results revealed an early and rapid loss of EBV from infected NPE cells during the period 12–72 h post-infection. Our independent experiments showed that the early and rapid loss of EBV could also be observed in NPE cells without TGF-β1 pretreatment, as exemplified by the data in Fig. S1. The reasons for this rapid loss of EBV at the early stage of infection are unclear, but inefficient replication of EBV in infected NPE cells and mis-segregation of EBV during cell division as well as the growth disadvantage of freshly infected cells may contribute. The slowing rate of EBV loss during the period 96–144 h post-infection (Fig. 3) suggests adaptation of EBV in infected NPE cells as well as adaptation of NPE cells to EBV infection.

EBV-infected NPE cells delay cell cycle entry immediately after infection

It was of interest to examine the fate of EBV-infected NPE cells at an early stage of infection, which has not been investigated before due to the lack of an efficient cell-free EBV infection system of epithelial cells. We monitored the effect of EBV infection on cell cycle entry on the single cell basis using live cell imaging of NP460hTert cells. Our experiments showed that most of the EBV-infected NP460hTert cells expressed GFP 48 h after infection. The EBV-infected NPE cells expressing GFP signals and uninfected cells in the same culture plates were monitored for an additional 60 h at 20-min intervals 48 h after EBV infection. A total of 161 initial EBV-infected and 169 uninfected cells were followed by live cell imaging and analysed. As shown in Fig. 5, we observed a delay in entering mitosis of NPE cells after EBV

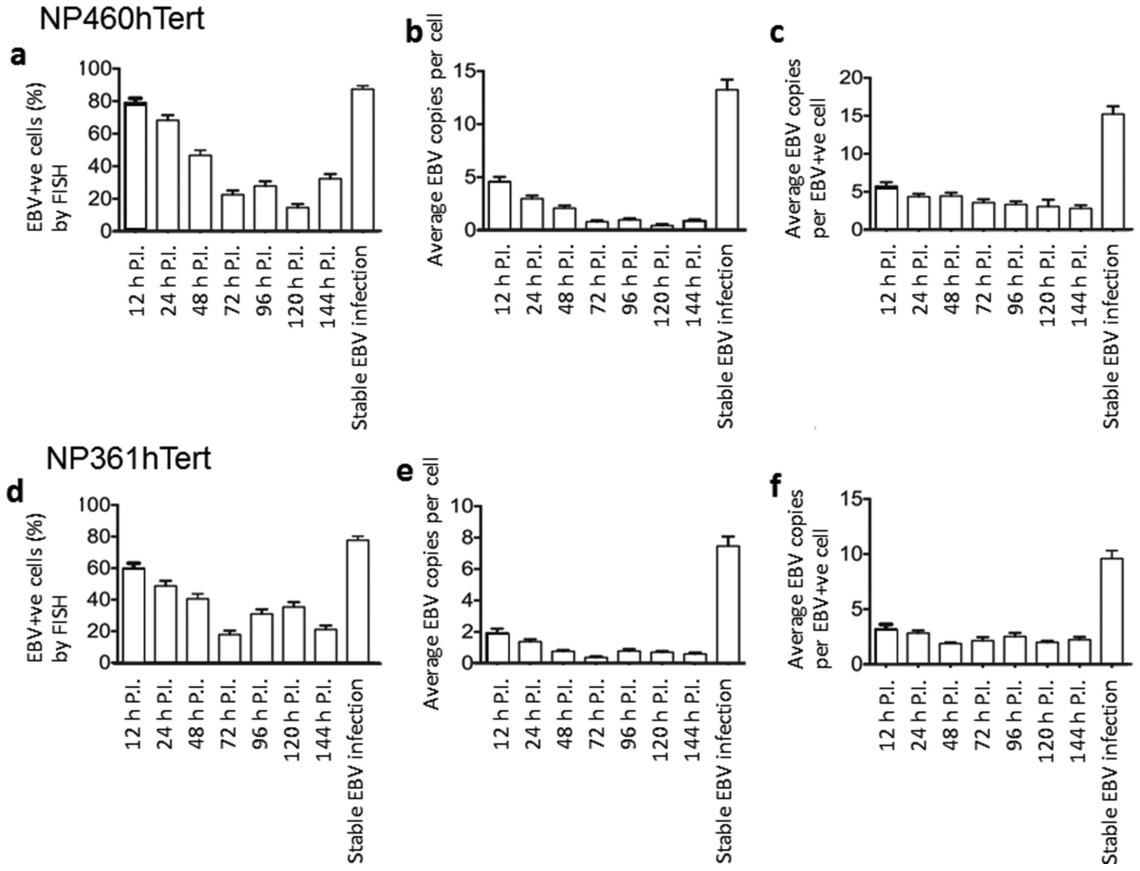

Fig. 3. Dynamic changes in the percentages of EBV-infected cells and average EBV copy numbers determined using EBV FISH. Stable EBV-infected cells were analysed for comparison. The stable EBV infection in immortalized NPE cells after cell-free infection was established as described in the Methods. (a,b,c) Dynamic changes in the percentage of EBV-positive NP460hTert cells, average EBV copies per cell and average EBV copies per EBV-positive cell, respectively, at different time points post-infection with EBV at an MOI of 3. (d,e,f) Dynamic changes in the percentage of EBV-positive NP361hTert cells, average EBV copies per cell and average EBV copies per EBV-positive cell, respectively, at different time points post-infection. Error bars in (a) and (d) represent standard deviations of the proportions. Error bars in (b), (c), (e) and (f) represent standard errors of the means analysed in more than 100 cells.

infection. The average duration of interphase from the start of imaging to entry into the first mitosis of EBV-infected cells was ~25 h compared with ~15 h in uninfected cells (P<0.05) (Fig. 5c). However, the average interval between the first and second mitosis of EBV-infected cells did not differ significantly from that of uninfected cells (Fig. 5d). These results suggest that the early delay in mitosis entry of NPE cells shortly after EBV infection may reflect a response of infected NPE cells to cellular stress associated with fresh EBV infection.

Establishment of stable EBV infection in immortalized NPE cells by cell-free infection

In both NP361hTert and NP460hTert cells, the percentages of EBV-positive cells decreased rapidly during the period 12–72 h after EBV infection, but the rate of decrease stabilized after 72 h post-infection (Fig. 3). This may suggest that a small proportion of EBV-infected NPE cells capable of supporting long-term EBV infection had emerged at the later period of infection. Indeed, by using single-cell plating, we could observe proliferative clones of dividing GFP-positive NP460hTert cells approximately 10 days after the cell-free mode of EBV infection (Fig. S3a), which were similar to the proliferative EBV-infected clones in the cell-to-cell contact mode of infection (Fig. S3b). We previously reported that $p16^{INK4a}$ loss or cyclin D1 overexpression supports stable EBV infection after multiple rounds of sorting for EBV-infected NPE cells using cell-to-cell contact-mediated EBV infection [7]. In the present study, we also attempted to achieve stable EBV infection of NPE cells using cell-free EBV infection. After each round of sorting for GFP-positive cells, the EBV-infected NPE cells were expanded for ~10–15 days, and then sorted again by FACS. After the 6th and 3rd round of sorting of NP460hTert and NP361hTert cells, respectively, the percentages of GFP-positive cells after expansion became stabilized, indicating successful selection of stably infected NPE cells using the cell-free mode of EBV infection (Fig. 6). Using EBV FISH analysis, we observed

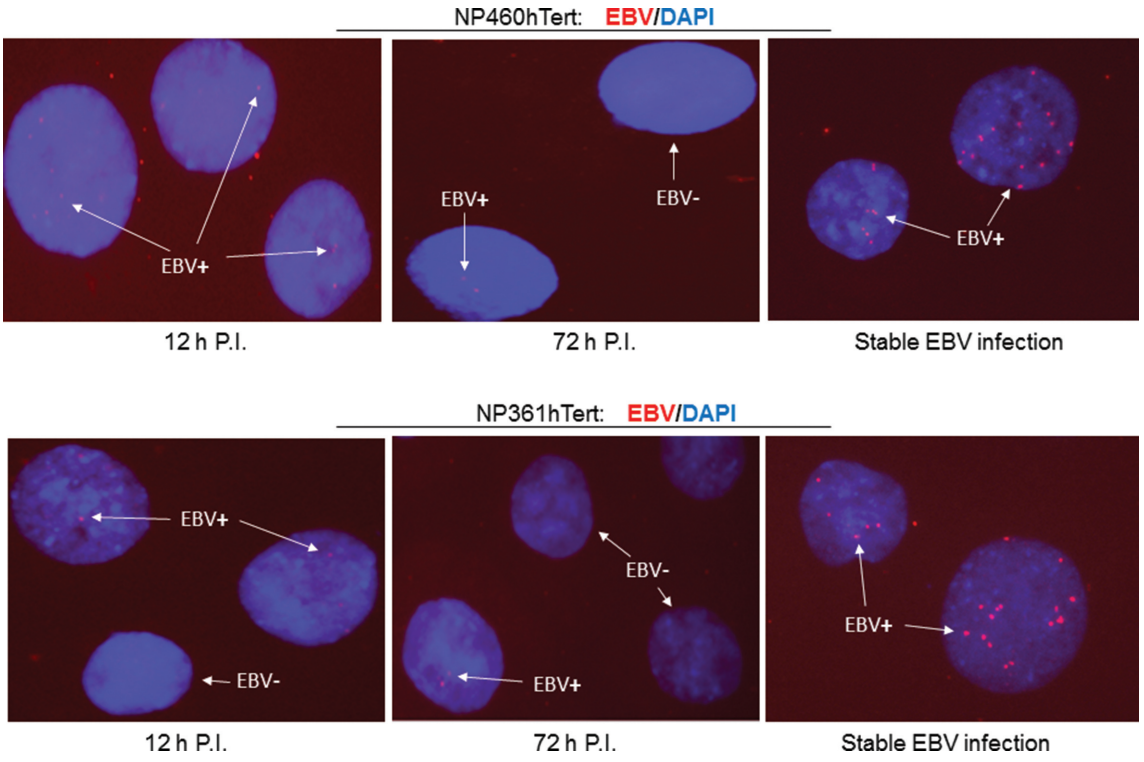

Fig. 4. Typical EBV FISH images in freshly and stably infected NP460hTert and NP361hTert cells. Red signals represent EBV copies. Cellular DNA was stained with DAPI (blue). EBV+ indicates an EBV-positive cell, and EBV- indicates an EBV-negative cell. Only the EBV copies in the nuclei were counted for EBV copy quantification.

that ~80 % of cells remained EBV-positive after propagation for 2 months (Fig. 3a, d), demonstrating stable EBV infection in both cell lines. We further analysed EBV FISH signal localizations on metaphase chromosomes in stably infected NP460hTert and NP361hTert cells. As shown in representative images of EBV FISH in Figs S4 and S5, the majority of EBV signals were non-symmetrically localized on sister chromatids, suggesting that most, if not all, EBV genomes in stably infected NPE cells were not integrated into host genomes. Hence, the cell-free EBV infection protocols for NPE cells established in this study could be used to reproducibly establish stable EBV-infected epithelial cell lines for further investigations.

Expression of EBV-encoded genes in freshly and stably EBV-infected NPE cells

The high efficiency in EBV infection of NPE cells by our cell-free infection method provided us a unique opportunity to carry out quantitative analysis of EBV gene transcription at the early stage of EBV infection in NPE cells without contamination of EBV-producing B cells (Fig. 7). The earliest time point we chose to analyse was 12 h after EBV infection when EBV has reached the nuclei of infected cells, as indicated by the expression of GFP in infected cells. Among the EBV-encoded genes we analysed, we did not detect significant transcription of lytic EBV genes *BZLF1*, *BRLF1*, *BMRF1* or *BLLF1* in the stably EBV-infected NPE cells. In contrast, the transcription of immediate early lytic EBV gene *BZLF1* and early lytic gene *BMRF1* were readily detected at various levels at early time points (12–72 h post-infection) in both freshly infected NPE cell lines. Notably, relatively high levels of *BZLF1* transcription were observed at 120 h post-infection in NP361hTert cells but low levels in NP460hTert cells, whereas *BRLF1* transcription was detected at relatively high levels at the early time points (12–72 h post-infection) in NP460hTert cells yet not in NP361hTert cells, which may reflect differences in the cellular contexts of the two cell lines that may affect EBV gene transcription. Transcription levels of the late lytic EBV gene *BLLF1* were insignificant in NP361hTert cells and at low levels in NP460hTert cells after fresh EBV infection. It appears that the immediate early lytic EBV genes were transcribed at an early stage of EBV infection in NPE cells but silenced in stably infected NPE cells. Moreover, the transcriptional profiles of latent EBV genes including *EBNA1*, *EBNA2*, *EBNA-LP*, *LMP1* and *LMP2* were also analysed and compared between freshly and stably infected NPE cells (Fig. 7). The expression profiles of *EBNA1* and *EBNA2* were of particular interest. The transcription level of *EBNA1* in stably infected NP361hTert cells was much higher than those in freshly infected NP361hTert cells; however, this pattern of transcription was not observed in infected

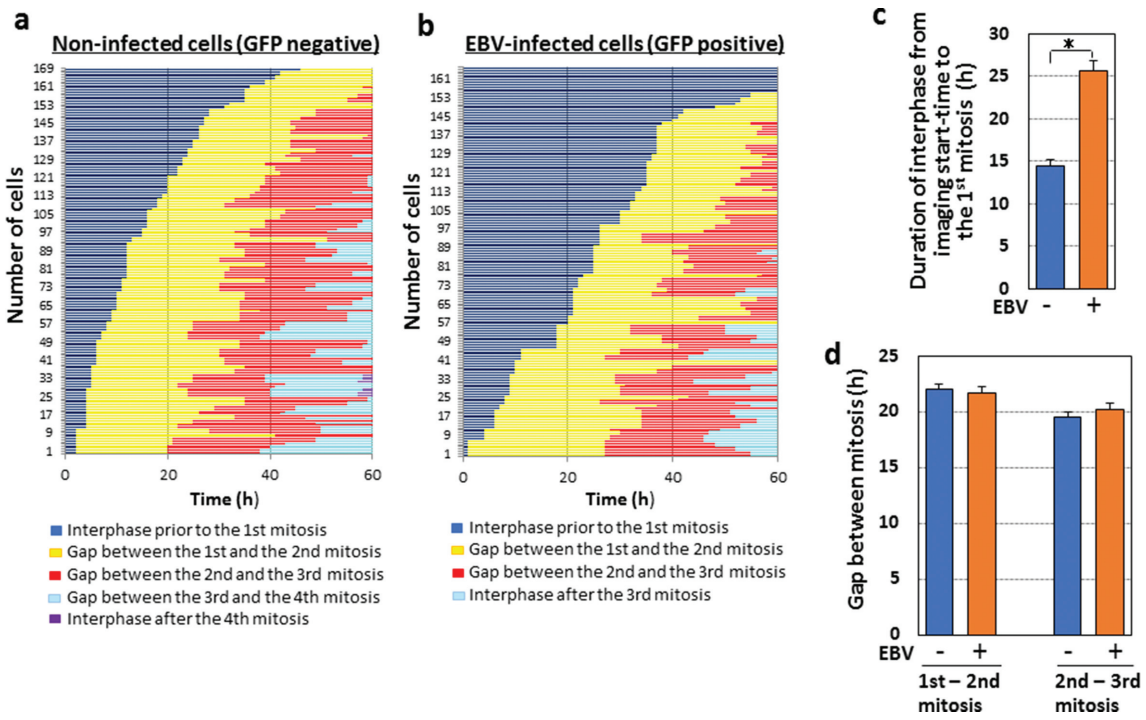

Fig. 5. Live cell imaging of cell-free EBV-infected NP460hTert cells. GFP-negative (uninfected) cells or GFP-positive (EBV-infected) cells in the same plate were imaged simultaneously for 60 h with an interval of 20 min. The fates of GFP-negative cells (n=169) (a) or GFP-positive cells (n=161) (b) were followed and recorded. Imaging was as described in the Methods. The statistical data from (a) and (b) are presented in (c) and (d). (c) The average duration of interphases from the start of imaging until the observed first mitoses of GFP-negative or GFP-positive cells. (d) The average time gaps between the 1st mitoses and the 2nd mitoses, and between the 2nd mitoses and the 3rd mitoses. In (c) and (d), errors bars represent standard errors. *Significant difference (P<0.05) between EBV-infected and uninfected cells.

NP460hTert cells, suggesting variations of cell context may influence viral gene expression. The transcription of *EBNA2*, which is a latent EBV gene normally expressed in EBV-infected B cells, was detected 12–144 h post-infection in both NPE cell lines, but not in stably EBV-infected NPE cells. We also detected low levels of *EBNA-LP* transcription in freshly infected NPE cells but not in stably infected NPE cells. Transcription of the latent EBV gene *LMP2*, which is commonly expressed in NPC cells, was detected at very low levels (barely detectable) in both freshly and stably infected cells of both NPE cell lines, which may also be related to the different intrinsic properties in NPE and NPC cells. A common observation regarding *LMP1* is that its transcription levels in both freshly infected NPE cell lines were consistently lower than those in stably infected NPE cells.

The above results may indicate that type II latent EBV infection, typically observed in EBV-associated epithelial cancers, is only established at a later stage in stably infected NPE cells. This is in line with the patterns of usage of the viral promoters Wp, Cp and Qp in EBV-infected NPE cells (Fig. 8a). Specifically, only transcription of the Qp promoter was detected in stably infected NPE cell lines. The Wp promoter was transcribed at steady levels 12–144 h post-infection in NP460hTert cells. In EBV-infected NP361hTert cells, the Wp promoter was transcribed at a relatively low level at 12 h post-infection, then at increased levels during the period 24–72 h, followed by decrease in transcription during the 96–144 h post-infection period. Transcription of the Cp promoter was periodically detected at low levels during the 12–144 h post-infection period in NP361hTert cells, but not detected during the 12–72 h post-infection period and at increasing levels during the 96–144 h post-infection period in NP460hTert cells. For comparison, Wp transcription was detected in EBV-superinfected Akata cells at 12 h post-infection; transcriptions of Cp and Qp were detected in B95.8 cells, consistent with a previous report [8]. The transcription levels of *EBER1/2* were detected at much lower levels at all post-infection time points examined in freshly infected NPE cells compared to stably EBV-infected NPE cells (Fig. 7). We also attempted to examine profiles of BART-microRNA expression in freshly and stably infected NPE cells, but they were expressed at very low levels and may not be accurate for comparative purposes (data not shown).

Western blotting analyses were carried out to examine whether the time courses of mRNA expression of some key

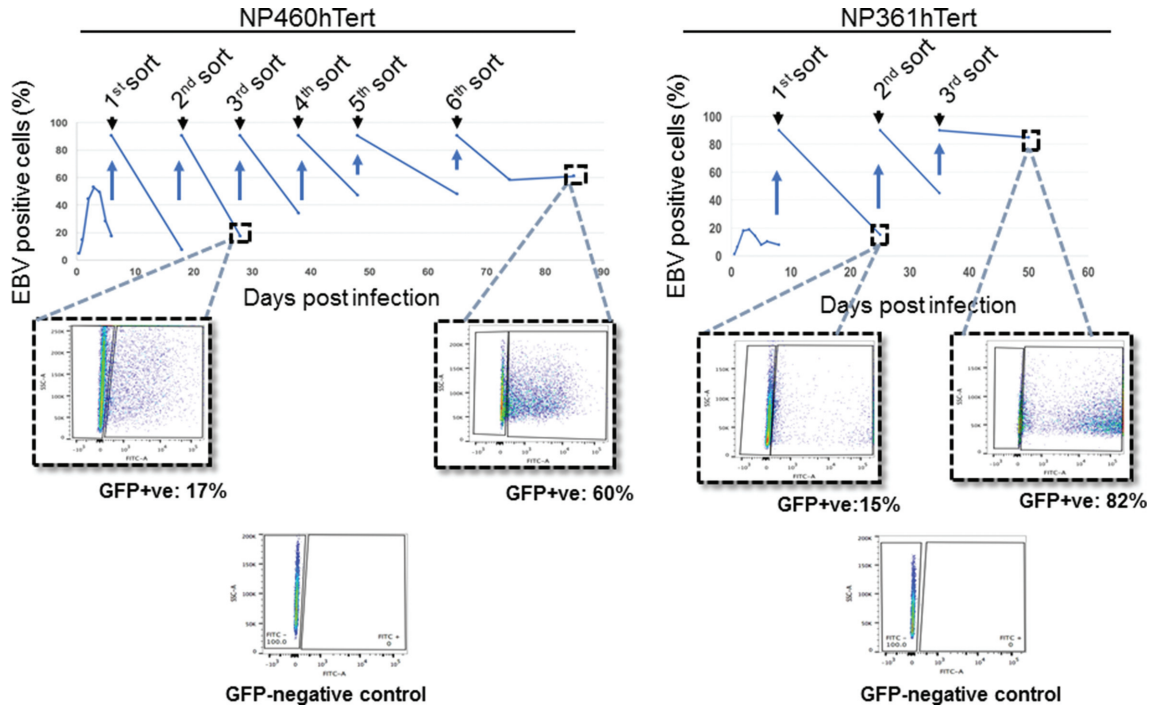

Fig. 6. Establishment of stable EBV infection in NPE cells by multiple rounds of sorting after the cell-free mode of EBV infection. The percentages of EBV-positive (GFP-positive) cells were analysed by flow cytometry. The blue curves and lines indicate the dynamic changes in the percentages of EBV-positive cells over time of cell culture. The upward blue arrows indicate cell sorting to enrich the EBV-positive cells. The dotted line squares show examples of the distributions of cell counts with different GFP intensities (blue dots). The background fluorescence distributions (EBV-negative controls) for NP460 and NP361 cells are shown in plots at the bottom. For NP460hTert cells, after the 6th round of sorting, the percentage of EBV-infected (GFP-positive) cells became stabilized (~60 %) about 10 days after sorting when compared with the percentage of EBV-infected cells (~60 %) after an additional 10 days of propagation. For NP361hTert cells, after the 3rd round of sorting, the percentage of EBV-infected (GFP-positive) cells became almost stabilized 15 days after the sorting (82 %) when compared with the initial percentage of GFP-positive cells (~90 %) immediately after sorting.

EBV genes correlated with their protein expression levels. As expected, stably EBV-infected NPE cells expressed undetectable or very low levels of lytic EBV proteins Zta and Rta (Fig. 8b). Somewhat unexpectedly, we did not detect significant levels of Zta and Rta expression in freshly infected NP361 and NP460hTert cells. As a positive control, stably EBV-infected Akata cells after treatment with anti-IgG antibody (inducing EBV lytic reactivation) expressed high levels of Zta and Rta. Freshly infected NPE cells also expressed undetectable or low levels of EBNA1 and LMP1 proteins in contrast to their remarkably higher levels of expression in stably infected NPE cells, and Akata and C666-1 cells. EBNA2 protein was not detected in freshly or stably infected NPE cells and C666-1 cells but was readily detected in B95.8 cells. Overall, the freshly infected NPE cells expressed very low or undetectable levels of the lytic and latent EBV proteins, which matched poorly with mRNA expression patterns of the EBV genes examined.

DISCUSSION

The development of a highly efficient cell-free EBV infection method in NPE cells allowed us to examine the early dynamic events involved in EBV infection of NPE cells without the contamination of B cells, for the first time. Previous major challenges to defining these events were possibly due to the low infection efficiency in cell-free EBV infection and the difficulty in completely removing the EBV-producing B cells from infected epithelial cells in the cell-to-cell contact mode of infection. Establishment of this highly efficient cell-free infection system will facilitate future research into important issues relating to the establishment of persistent EBV infection in NPE cells, which are the relevant target cell type for functional studies of EBV in the pathogenesis of NPC.

Several novel findings from this study may have important implications for understanding the dynamic events leading to establishment of latent EBV infection in NPE cells. First, by using EBV FISH, we observed a quick decrease in the percentage of EBV-positive NPE cells starting from the first day after infection. Specifically, when measured at 24 h post-infection, average EBV copy numbers per cell dropped to ~70 % of that in NP460hTert cells during the 12 h post-infection period, and this trend of decrease continued until 72 h post-infection. A similar trend of decrease in EBV copy

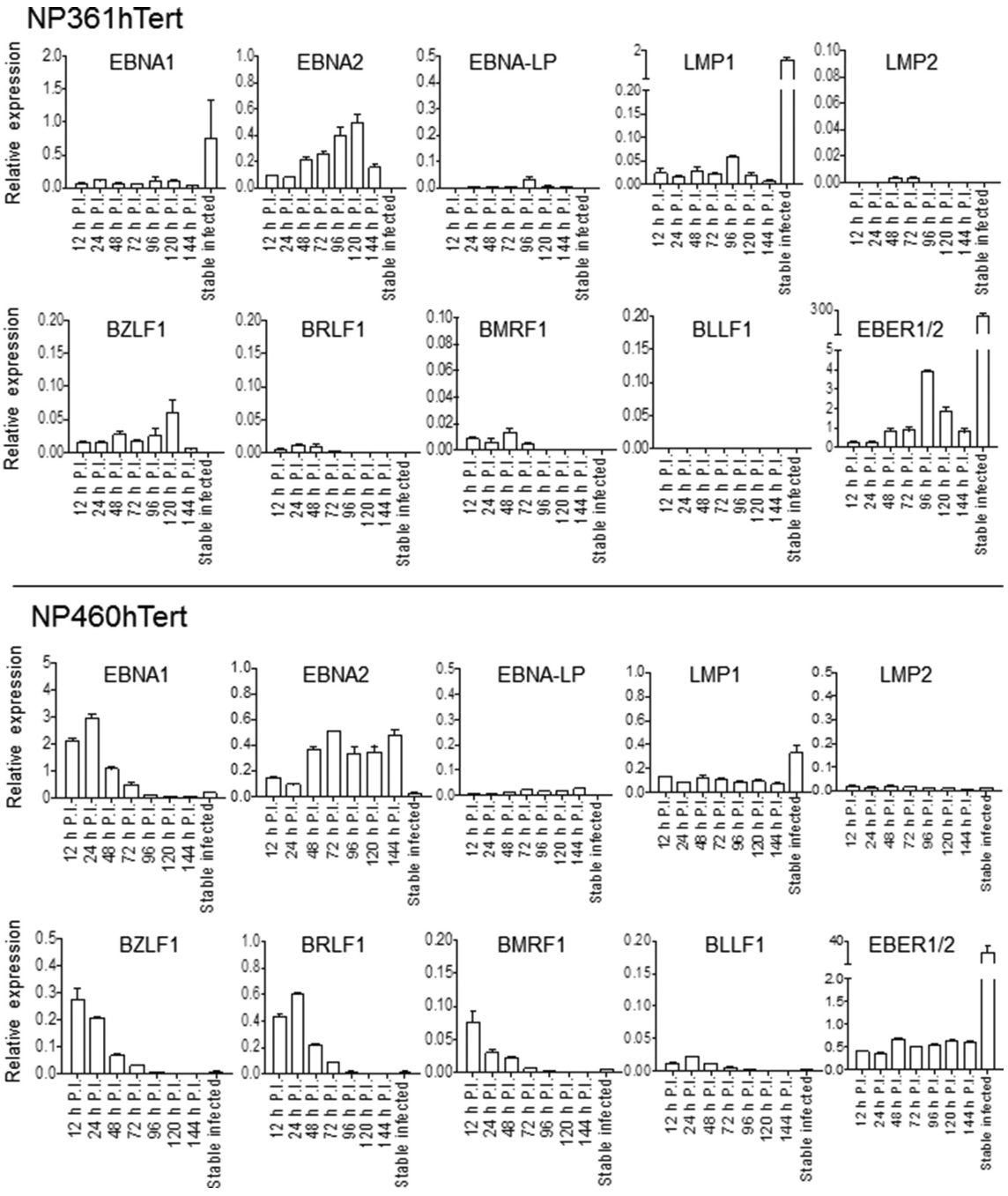

Fig. 7. Dynamic changes in EBV gene expression (mRNA transcripts) profiles in freshly infected NP361hTert and NP460hTert cells. Stable EBV-infected cells were also analysed for comparison. EBV gene transcripts are displayed as relative expression levels (relative to GAPDH, ×1000). Error bars represent standard deviations for triplicate measurements.

numbers per cell was also observed in EBV-infected NP361hTert cells. To the best of our knowledge, this is the first time that such an early and quick loss of EBV was revealed and documented in EBV-infected epithelial cells. Although in our routine EBV infection experiments MOI values of about 1–3 were used for NPE cells, we also examined the dynamics of EBV loss from NPE cells after EBV infection with lower MOI.o.i. values (0.25–0.5) and found a similar trend of EBV loss in freshly infected NPE cells (data not shown). This might be due to the delayed entry of EBV-infected cells into the cell cycle as well as inefficient EBV replication in freshly infected NPE cells. In previous studies using other epithelial cell models, a trend of precipitous loss of *oriP* plasmids and EBV genomes was reported 3 days

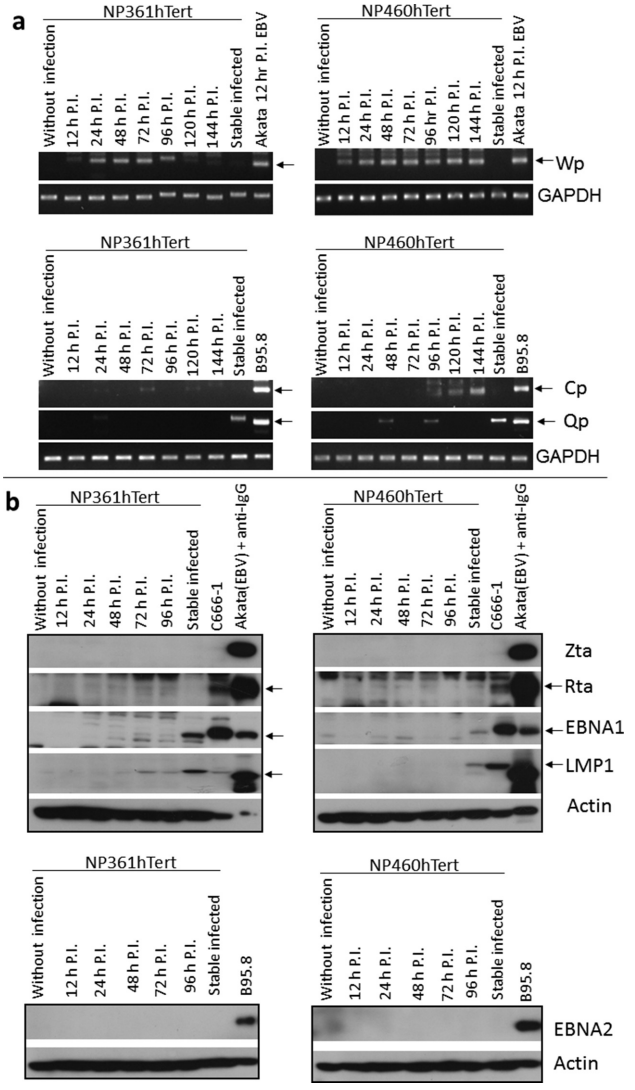

Fig. 8. EBV promoter transcription and Western blotting analyses. (a) Semi-quantitative PCR analysis for EBV promoters. NPE cells without EBV infection served as negative controls. Arrows indicate the specific bands for analysis of transcription levels. For Wp, Akata cells at 12 h after fresh EBV infection were used as the positive control. For Cp and Qp, B95.8 cells were used as the positive control because both promoters are known to be activated in B95.8 cells [8]. GAPDH served as a PCR control. (b) Western blotting analysis for key EBV protein expressions. Arrows indicate the specific bands for analysis of the protein expression levels. For *Zta* and *Rta* detection, Akata cells with stable EBV infection treated with anti-IgG antibody (inducing EBV lytic reactivation) served as the positive control. For *EBNA1* and *LMP1* detection, C666-1 and Akata cells with stable EBV infection served as positive controls. For *EBNA2* detection, B95.8 cells were used as the positive control. Actin served as a protein loading control.

after introduction into the cells either by infection or transfection [4, 9]. It is particularly noteworthy that during the 72–144 h period after infection of NPE cells, the rate of EBV copy loss decreased compared with the earlier time points. Apparently, there was a process of adaptation of EBV in the infected NPE cells as well as adaption of host NPE cells to EBV infection, eventually leading to establishment of stably infected NPE cells. The molecular and cellular events mediating these adaption processes are largely unclear at this stage.

Second, we observed that transcription of EBV lytic genes, *BZLF1* and *BMRF1*, was detected at relatively high levels at an early stage (12–72 h) post-infection in both NPE cell lines. Transcription of lytic EBV genes was generally silenced in stably infected NPE cells. The immediate-early EBV lytic gene *BRLF1* was also transcribed at relatively high levels in freshly infected NP460hTert cells, but at relatively lower levels in freshly infected NP361hTert cells. TGF-β1 has been reported to induce EBV lytic reactivation in B cells [10]. We examined if there was truly lytic reactivation of EBV in freshly infected NPE cells. Supernatant collected from the infected NPE cells did not result in the appearance of GFP-positive clones after incubation with EBV-negative Akata cells (data not shown). Furthermore, we did not observe the appearance of lytic replication compartments using EBV FISH (data not shown), which would be characterized by numerous EBV copies detectable within discrete sites in nuclei of EBV-infected NPE cells. As a positive control, the appearance of EBV lytic replication compartments could be readily demonstrated in EBV-infected HONE1 cells after ectopic expression of *BZLF1* in EBV-superinfected HONE1 cells as reported in our previous study [11]. Moreover, transcription of the late EBV lytic gene *BLLF1*, which encodes a key component (gp350) of the protein coat of EBV, was not detected at significant levels in freshly infected NPE cells. Of note, expression levels of Zta and Rta, the major lytic proteins encoded by the *BZLF1* and *BRLF1* genes, respectively, as detected by Western blotting analysis were very low or undetectable in freshly infected NPE cells. Together, these results indicate that there was no functional lytic reactivation of EBV in freshly infected NPE cells despite some transcription of mRNA of the lytic EBV genes.

Third, transcription of *EBER1/2* (EBV-encoded small RNA) could be detected in freshly infected NPE cells. Strikingly, stable EBV-infected NPE cells transcribed *EBER1/2* at a dramatically higher level compared to freshly infected cells. These results imply that the high levels of *EBER1/2* transcription may play a functional role in the long-term persistence of EBV infection in NPE cells. *EBER1/2* has been shown to inhibit cellular apoptosis [12, 13] and regulate cellular signalling pathways to promote cellular survival, conferring a growth advantage to stable EBV-infected cells under stressful conditions [14].

Fourth, the *EBNA1* transcription (mRNA) levels at some time points in freshly infected NP460hTert cells were higher than that in stably EBV-infected NP460hTert cells, yet expression levels of *EBNA1* proteins in freshly infected NPE cells detected by Western blotting analysis were low or undetectable. In contrast, markedly higher levels of *EBNA1* protein expression were detected in stably EBV-infected cells. The *EBNA1* protein is required for replication of EBV

during latent infection and for tethering EBV DNA to host chromosomes to facilitate segregation of EBV genomes during mitosis. The low levels of *EBNA1* protein expression in freshly infected NPE cells provide an explanation for the rapid loss of EBV copies from freshly infected cells.

An additional unexpected finding from this study was that *EBNA2* was transcribed at relatively high levels in freshly infected NPE cells of both cell lines, but was completely silenced in stably infected NPE cells. Although *EBNA2* is known to be essential for B cell transformation, it is not expressed in NPC cells [1]. The fact that we detected *EBNA2* in freshly infected NPE cells but not in stably infected NPE cells suggested that the EBV episomes in freshly infected NPE cells have not been epigenetically modified to establish the typical latent programme of EBV infection observed in NPC cells. The regulation and usage of EBV promoters have been much better defined in infected B cells than in epithelial cells. In our NPE cell models, we detected Wp and Cp promoter transcriptions in freshly infected cells, which may explain the transcription of the *EBNA2* and *EBNA-LP* genes in those cells. However, in stably EBV-infected NPE cells, only the Qp promoter was turned on (Fig. 8a). Our EBV-infected cells could serve as relevant cell models to further study this virus–host interaction.

Another novel and important finding from this study is that the transcripts of EBV latent and lytic genes were not efficiently translated into protein in freshly infected NPE cells, for reasons that are not yet clear. This may reflect an immediate innate response of host cells to fresh EBV infection or selection of a specific host cellular microenvironment essential for efficient protein translation of EBV latent gene transcripts to support persistent EBV infection. Establishment of the cell-free infection system will enable further investigation of the regulation of viral gene expression in epithelial cells.

In this study, we consistently observed a rapid loss of EBV episomes in NPE cells immediately after infection. An earlier study using EBV *oriP* plasmids also showed precipitous loss of the newly transfected plasmids from epithelial cells, and the loss was not related to genetic mutations within the plasmids [9]. Similar to the retention of EBV genomes observed in our stably infected NPE cells, the *oriP* plasmids could also be stably maintained in recipient epithelial cells after repeated rounds of selection, and epigenetic changes in *oriP* were suggested to be involved in efficient replication and stable maintenance of the plasmids in infected cells [9]. The *oriP* consists of two basic elements: the family of repeats (FR) and dyad symmetry (DS) element. The initiation of DNA synthesis for latent EBV replication occurs at or near the DS element of *oriP*. However, the FR element, which is essential for EBV partition, forms a severe barrier for DNA synthesis from *oriP* in certain cell lines [9, 15, 16]. Epigenetic changes leading to elimination of this inhibitory function of FR in *oriP* synthesis are required for the efficient latent replication of *oriP* [9, 16]. Taking this evidence together, we speculate that epigenetic modifications of EBV genomes including *oriP* and alterations of the cellular microenvironment are involved in establishment of stable infection of EBV in NPE cells, which requires efficient latent replication and proper partition of EBV. The hypothesized epigenetic changes in EBV genomes warrant further research and are currently under investigation in our laboratories.

Previous studies, including ours, have shown that EBV infection *per se* does not confer a growth advantage to epithelial cells [4, 7, 17, 18]. In this study, we observed an initial delay in cell cycle entry immediately after EBV infection. One of the reasons for this may be the initial linearized nature of EBV genomes entering into host cells. This may trigger a DNA damage response in host cells at the early stage of EBV infection [18]. Presumably, the circularization of EBV episomes only occurs at the later stage of EBV infection, leading to stable EBV infection in epithelial cells, a process which warrants further investigation. In NPC patients, EBV is present in virtually all cancer cells in the tumours, suggesting a strong selection force and survival advantage of EBV-infected NPC cells *in vivo*. EBV infection may provide an advantage for EBV-infected NPC cells *in vivo* through immune evasion (which is absent in the *in vitro* environment) and suppression of apoptosis under harsh conditions [19, 20]. Defining the nature of this selective force will provide important clues to the role of EBV infection in NPC. Establishment of efficient EBV infection protocols for NPE cells will facilitate further research into these important issues in the early pathogenesis of NPC.

In conclusion, by taking advantage of our highly efficient cell-free EBV infection method in NPE cells, we were able to reveal, for the first time, aspects of the dynamics of EBV infection and viral gene expression at an early stage of EBV infection. Strikingly, differences in the profiles of EBV gene expression and the maintenance of EBV copies were revealed between stably and freshly infected NPE cells. The efficient cell-free EBV infection of NPE cells and stable establishment of EBV-infected NPE cell lines will facilitate investigation into the dynamic events at an early stage of EBV infection of premalignant NPE cells, leading to establishment of stable and latent EBV infection, which is an essential step in NPC development.

METHODS

Cell lines and cell culture

NPE cell lines (NP361hTert, NP460hTert and NP550hTert) were immortalized by the catalytic subunit of telomerase, hTert [5–7]. Both EBV-infected and non-infected Akata cell lines were kindly provided by Prof. Kenzo Takada (Hokkaido University School of Medicine, Sapporo, Japan). All immortalized NPE cell lines were cultured with Defined Keratinocyte-SFM (Gibco) and EpiLife medium (Cascade Biologics) at a ratio of 1 : 1 (hereafter D+E medium) containing growth supplements, while other cell lines were cultured with RPMI 1640 medium (Sigma) supplemented with

10 % FBS (Gibco). Recombinant EBV-infected Akata cells were treated with G418 (600 μg ml^{-1}; Gibco). All cell lines were incubated in a humidified incubator at 37 °C with 5 % CO_2.

EBV infection of NPE cells

The immortalized NPE cells were infected with GFP-tagged EBV harvested from EBV-harbouring Akata cells, which were induced to undergo EBV lytic reactivation by treatment with anti-IgG antibody (Sigma, 5 μg for 2×10^6 EBV-infected Akata cells per millilitre). For the cell-to-cell contact mode of infection, anti-IgG antibody treatment of EBV-harbouring Akata cells for 24 h was adequate; for cell-free infection, 5 days of anti-IgG antibody treatment was needed for the production of higher titres of EBV. NPE cells were either co-cultured directly with the EBV-reactivated Akata cells (cell-to-cell mode of infection) or cultured with EBV-containing supernatant (cell-free mode of infection). The cell-to-cell contact mode of EBV infection between EBV-producing Akata cells and epithelial cells was performed according to the protocols published in previous studies [5, 7]. Briefly, NPE cells were seeded in a six-well plate with 1×10^5 cells per well and cultured with D+E medium for 24 h. TGF-β1 (2 ng ml^{-1}; CalBiochem) was added into the medium and incubated for another 24 h. The TGF-β1-containing medium was then discarded and replaced with 1.5 ml fresh medium per well, followed by addition of 1.5 ml of EBV-reactivated Akata cell suspension into the epithelial cell culture. We choose to use TGF-β1 at 2 ng ml^{-1} in our routine EBV infection experiments because this is well within the physiological range of active TGF-β1 (0.03–4.0 ng ml^{-1}) [21, 22] and it is easy to achieve the final concentration from stock solution for long-term stable storage of TGF-β1. The cells were co-cultured for 48 h at 37 °C. Then, EBV-reactivated Akata cells were removed, and the epithelial cell cultures were washed thoroughly with 1× PBS four or five times. The NPE cells were examined for EBV infection (expression of GFP) after 2 days. In our experience, it is difficult to completely remove the EBV-reactivated Akata cells from the culture as some of the Akata cells formed stable conjugates with the co-cultured NPE cells. The presence of 'contaminating' Akata cells will interfere with the accurate detection of EBV gene expression and quantification of EBV copies. For accurate determination of these dynamic events at an early stage of infection, a cell-free infection approach was developed. For cell-free infection, supernatant (~40 ml) collected from the cultures of EBV-reactivated Akata cells (after treatment with anti-IgG antibody for 5 days) was filtered through a 0.45-μm pore-sized filter (Iwaki) and centrifuged at 27,600 RCF for 3 h at 4 °C to pellet the EBV. The pelleted EBV virions were re-suspended in 10 % FBS-supplemented fresh RPMI medium to produce a 10-fold concentrated EBV suspension, which was stored at 4 °C for cell-free EBV infection. The EBV titres were estimated by the number of Raji cells infected (green Raji unit, GRU). To perform cell-free EBV infection, NPE cells were seeded in a six-well plate with 1×10^5 cells per well and cultured for 24 h in 2 ml of D+E medium. For routine EBV infection of NPE cells, TGF-β1 (2 ng ml^{-1}; CalBiochem) was added to the medium and the cells were cultured for another 24 h (cell number increased to ~3×10^5 cells per well). TGF-β1-containing medium was replaced with 2 ml of fresh D+E medium. For some experiments testing the effects of TGF-β1 on EBV infection efficiency, the TGF-β1 addition step was skipped for comparison. In each well of epithelial cells, 1.5 ml of 10-fold concentrated cell-free EBV virion suspension containing ~1×10^6 GRU was added. The culture plate was subjected to centrifugation at 2465 RCF at 37 °C for 1 h. The culture plate was transferred carefully back to the incubator and incubated for 12 h before being replaced with fresh D+E medium. The EBV-infected NPE cells were harvested at different time points post-infection for detection and estimation of EBV-infected (GFP-positive) cells using a flow cytometer (LSR Fortessa Analyzer; BD Biosciences). Quantification of EBV copy number was performed by FISH analysis and EBV gene transcription analysis by RT-PCR using specific PCR primers.

EBV copy number analysis by FISH

Cell spreading on slides and EBV FISH were performed as previously reported [7, 23]. Briefly, a 7-day slide was treated at 37 °C with 0.1 mg ml^{-1} RNase (DNase-free) and 0.025 μg ml^{-1} proteinase K for 1 h and 15 min, respectively, washed with 2× SSC, fixed with 2 % paraformaldehyde for 10 min at room temperature, washed again with 2× SSC for 10 min, dehydrated with 70 %, 85 % and 95 % ethanol for 2 min each, and air dried with nitrogen gas. The slide was placed in 70 % deionized formamide for 4 min at 80 °C, dehydrated with ethanol and air dried as above. For each sample, 4 μl biotin-labelled EBV probes (kindly provided by Prof. B. Sugden, University of Wisconsin, Madison) were denatured for 4 min at 80 °C, incubated for 30 min at 37 °C, and added onto the slide, which was then covered with a coverslip and sealed with rubber cement. The slide was incubated at 37 °C overnight, and washed with 50 % formamide and twice with 2× SSC for 5 min each at 45 °C. Then, 30 μl of Cy3-conjugated streptavidin (Cytocell) was added to the slide, which was then incubated for 30 min and washed twice with 2× SSC for 5 min at 45 °C, dehydrated with ethanol and air dried. DNA was counterstained by antifade-containing DAPI (Cytocell). Images were acquired using a Leica fluorescence microscope equipped with a CCD camera.

Flow cytometric analysis for EBV infection rate and cell sorting

For flow cytometric analysis, various EBV-infected and uninfected NPE cell lines were harvested and re-suspended in 1× PBS. Non-infected cells of each cell line were used to gate the viable cell fraction according to the granularity and size of the cells. Cells in suspension were analysed via an LSR Fortessa Analyzer (BD Biosciences) and the percentage of GFP-positive cells was quantified by using the Flowjo software version 7.0. For flow sorting of EBV-infected cells, EBV-infected NPE cell cultures were harvested and re-suspended in D+E medium. The EBV-infected cells (expressing

GFP) were purified from GFP-negative cells by using the FASC Aria II SORP cell sorter (BD Biosciences). Sorted EBV-infected cells were then seeded onto the culture plates and continuously propagated. The flow sorting of EBV-infected cells was carried out in multiple rounds to establish stable EBV-infected NPE cells.

Live cell imaging

EBV-infected NP460hTert cells were seeded onto multi-well flat bottom plates and subjected to wide-field imaging starting from 48 h after EBV infection, under a spinning disc microscope (ERS 20; Perkin Elmer) equipped with a CCD camera. The live cells were maintained at 37 °C in an incubator chamber with 5 % CO_2 supply and imaged on a motorized microscopic stage. Phase contrast and GFP fluorescence images were acquired with an interval of 20 min for 60 h (image acquisition time 200 ms). Initially, the cells to be imaged were chosen randomly, and the cell fates (including their daughter cells) were followed individually for 60 h. Mitoses were indicated by the appearance of rounding up. The time intervals between mitoses were recorded. Both GFP-positive and GFP-negative cells, representing EBV-infected and uninfected cells in the same culture plates, respectively, were monitored. For EBV-infected and uninfected cells, initially 161 and 169 cells and their daughter cells were followed, respectively. MetaMorph software (version 7.8.3.0) was used for image processing and cell division times were analysed manually.

Establishment of stable EBV infection in immortalized NPE cells by cell-free infection

Ten days after cell-free EBV infection, GFP-positive (EBV-positive) NPE cells were enriched by cell-sorting using a high-performance cell sorter (FACS Aria II SORP; BD). The GFP-positive cells were expanded for ~10–15 days. The expanded cells were then sorted again for GFP-positive cells by FACS. After the 6th and 3rd round of sorting of NP460hTert and NP361hTert cells, respectively, the percentages of GFP-positive cells as analysed using flow cytometry after 10–15 days of expansion became stabilized, indicating successful selection of stably infected NPE cells after cell-free EBV infection (Fig. 6).

EBV mRNA and miRNA transcription assay

EBV-infected NP460hTert and NP361hTert cells at different time points post-infection were harvested for RNA extraction using TRIZOL reagent (Invitrogen) and reversely transcribed to cDNA with random primers using a SuperScript II Reverse Transcriptase kit (Invitrogen). Expression levels of EBV mRNA transcripts were detected with quantitative real-time PCR using LightCycler 480 Probe Master with Universal ProbeLibrary Set, Human (Roche Applied Science) according to the company's protocols. Specific primers of the target genes were designed (ProbeFinder software) and the top-ranking primers with their corresponding probes used in this study are listed in Table S1. RT-PCRs were performed using a PE GeneAmp PCR system 9700 machine (PE Biosystem). EBV gene transcripts were displayed as gene expression relative to GAPDH (internal control, ×1000). Multiple stem-loop reverse transcription and quantitative real-time PCR were performed to determine the expression of EBV micro RNAs (miRNAs). The transcripts of each miRNA were detected with specific primer sequences. RT-PCRs for each target gene were performed in triplicate.

Semi-quantitative PCR for EBV promoters

RNA was extracted from non-infected, fresh EBV-infected and stably infected NPE cells. cDNAs were prepared with random primers using the SuperScript reverse transcription kit from Invitrogen. After reverse transcription, cDNAs were diluted with a dilution factor of 5. For each semi-quantitative PCR, 1 µl of diluted cDNA was used. The PCR programme consisted of 94 °C for 2 min, cycles of 94 °C for 45 s, 45 °C for 30 s and 72 °C for 1 min depending on the different promoters, and 72 °C for 10 min. For the Wp/Cp promoter, 40 cycles were enough for detection. For the Qp promoter, 50 PCR cycles were required. Primers used are listed in Table S2.

Western blotting

After EBV infection, cells were lysed in RIPA buffer with proteinase inhibitors and phosphatase inhibitor (Roche Applied Science). Protein concentration was determined by the DC protein assay (Bio-Rad). Ten micrograms of protein was separated by SDS-PAGE, transferred to a PVDF membrane and probed with specific primary antibodies. Rabbit monoclonal antibody against EBV EBNA1 (K67.3), and mouse monoclonal antibodies against EBV EBNA2 (PE-2) and LMP1 (OT21-C) were kindly provided by Prof. Jaap M. Middeldorp. Mouse monoclonal antibodies against EBV Zta and Rta were purchased from Argene. Mouse monoclonal antibody against involucrin (SY5) was from Thermo Fisher. Mouse monoclonal antibodies against cytokeratin 5/18 (C-50) and cytokeratin 18 (DC-10) were from Novocastra. Mouse monoclonal antibody against pan-keratin (AE1/AE3) was purchased from Dako. Mouse monoclonal against actin (C4) was from Santa Cruz. After incubation with species-specific HRP-conjugated secondary antibodies, the signal was developed by chemiluminiscence (SuperSignal West Femto maximum-sensitivity substrate) and blots were visualized on X-ray film.

Statistical analysis

A two-tailed *t*-test was used to examine statistical differences. *P* values <0.05 were regarded as significant.

Funding information
The authors acknowledge the generous funding sources for the above study: HMRF grant 260870784; and fundings from the Hong Kong Research Grant council: General Research Fund (HKU 779713M, 17106414 and 17116416), AoE NPC grant (AoE/M-06/08), Theme-based Research Scheme grant (T12-401/13 R) and Collaborative Research Grant (C7027-16G). The funders had no role in study design, data collection and interpretation, or the decision to submit the work for publication.

Acknowledgements
We thank Professor B. Sugden, University of Wisconsin, USA, and Professor J. Middeldorp, VU University Medical Center, Netherlands, for providing EBV DNA probes for FISH and EBV antibodies for Western blotting analysis, respectively. We also thank Professor K. Takada, Hokkaido University, Japan, for providing the EBV-infected or non-infected Akata cell lines. We thank the Faculty Core Facility (Li Ka Shing Faculty of Medicine, The University of Hong Kong) for supporting the imaging and flow cytometric studies.

Conflicts of interest
The authors declare that there are no conflicts of interest.

References
1. Young LS, Rickinson AB. Epstein-barr virus: 40 years on. *Nat Rev Cancer* 2004;4:757–768.
2. Pathmanathan R, Prasad U, Sadler R, Flynn K, Raab-Traub N. Clonal proliferations of cells infected with Epstein-Barr virus in preinvasive lesions related to nasopharyngeal carcinoma. *N Engl J Med* 1995;333:693–698.
3. Imai S, Nishikawa J, Takada K. Cell-to-cell contact as an efficient mode of Epstein-Barr virus infection of diverse human epithelial cells. *J Virol* 1998;72:4371–4378.
4. Shannon-Lowe C, Adland E, Bell AI, Delecluse HJ, Rickinson AB *et al.* Features distinguishing Epstein-Barr virus infections of epithelial cells and B cells: viral genome expression, genome maintenance, and genome amplification. *J Virol* 2009;83:7749–7760.
5. Tsang CM, Zhang G, Seto E, Takada K, Deng W *et al.* Epstein-Barr virus infection in immortalized nasopharyngeal epithelial cells: regulation of infection and phenotypic characterization. *Int J Cancer* 2010;127:1570–1583.
6. Li HM, Man C, Jin Y, Deng W, Yip YL *et al.* Molecular and cytogenetic changes involved in the immortalization of nasopharyngeal epithelial cells by telomerase. *Int J Cancer* 2006;119:1567–1576.
7. Tsang CM, Yip YL, Lo KW, Deng W, To KF *et al.* Cyclin D1 overexpression supports stable EBV infection in nasopharyngeal epithelial cells. *Proc Natl Acad Sci USA* 2012;109:E3473–E3482.
8. Tao Q, Robertson KD, Manns A, Hildesheim A, Ambinder RF. The Epstein-Barr virus major latent promoter Qp is constitutively active, hypomethylated, and methylation sensitive. *J Virol* 1998;72:7075–7083.
9. Leight ER, Sugden B. Establishment of an oriP replicon is dependent upon an infrequent, epigenetic event. *Mol Cell Biol* 2001;21:4149–4161.
10. Nanbo A, Ohashi M, Yoshiyama H, Ohba Y. The role of transforming growth factor β in cell-to-cell contact-mediated Epstein-Barr virus transmission. *Front Microbiol* 2018;9:984.
11. Hau PM, Deng W, Jia L, Yang J, Tsurumi T *et al.* Role of ATM in the formation of the replication compartment during lytic replication of Epstein-Barr virus in nasopharyngeal epithelial cells. *J Virol* 2015;89:652–668.
12. Ruf IK, Lackey KA, Warudkar S, Sample JT. Protection from interferon-induced apoptosis by Epstein-Barr virus small RNAs is not mediated by inhibition of PKR. *J Virol* 2005;79:14562–14569.
13. Wong HL, Wang X, Chang RC, Jin DY, Feng H *et al.* Stable expression of EBERs in immortalized nasopharyngeal epithelial cells confers resistance to apoptotic stress. *Mol Carcinog* 2005;44:92–101.
14. Iwakiri D, Eizuru Y, Tokunaga M, Takada K. Autocrine growth of Epstein-Barr virus-positive gastric carcinoma cells mediated by an epstein-barr virus-encoded small RNA. *Cancer Res* 2003;63:7062–7067.
15. Dhar V, Schildkraut CL. Role of EBNA-1 in arresting replication forks at the Epstein-Barr virus oriP family of tandem repeats. *Mol Cell Biol* 1991;11:6268–6278.
16. Leight ER, Sugden B, Light ER. The cis-acting family of repeats can inhibit as well as stimulate establishment of an oriP replicon. *J Virol* 2001;75:10709–10720.
17. Temple RM, Zhu J, Budgeon L, Christensen ND, Meyers C *et al.* Efficient replication of Epstein-Barr virus in stratified epithelium *in vitro*. *Proc Natl Acad Sci USA* 2014;111:16544–16549.
18. Lieberman PM. Keeping it quiet: chromatin control of gammaherpesvirus latency. *Nat Rev Microbiol* 2013;11:863–875.
19. Kang D, Skalsky RL, Cullen BR. EBV BART microRNAs target multiple pro-apoptotic cellular genes to promote epithelial cell survival. *PLoS Pathog* 2015;11:e1004979.
20. Saridakis V, Sheng Y, Sarkari F, Holowaty MN, Shire K *et al.* Structure of the p53 binding domain of HAUSP/USP7 bound to Epstein-Barr nuclear antigen 1 implications for EBV-mediated immortalization. *Mol Cell* 2005;18:25–36.
21. Dziadzio M, Smith RE, Abraham DJ, Black CM, Denton CP. Circulating levels of active transforming growth factor beta1 are reduced in diffuse cutaneous systemic sclerosis and correlate inversely with the modified Rodnan skin score. *Rheumatology* 2005;44:1518–1524.
22. Ayatollahi M, Geramizadeh B, Samsami A. Transforming growth factor beta-1 influence on fetal allografts during pregnancy. *Transplant Proc* 2005;37:4603–4604.
23. Deng W, Tsao SW, Lucas JN, Leung CS, Cheung AL. A new method for improving metaphase chromosome spreading. *Cytometry A* 2003;51:46–51.